The AAPS Journal (2022) 24: 91
https://doi.org/10.1208/s12248-022-00733-x

RESEARCH ARTICLE

Determination of the Number of Tissue Groups of Kinetically Distinct Transit Time in Whole-Body Physiologically Based Pharmacokinetic (PBPK) Models II: Practical Application of Tissue Lumping Theories for Pharmacokinetics of Various Compounds

Yoo-Seong Jeong[1] · Min-Soo Kim[1] · Suk-Jae Chung[1]

Received: 4 April 2022 / Accepted: 5 July 2022 / Published online: 24 August 2022

Abstract
In our companion paper, we described the theoretical basis for tissue lumping in whole-body physiologically based pharmacokinetic (WB-PBPK) models and found that K_{det}, a coefficient for determining the number of tissue groups of distinct transit time in WB-PBPK models, was related to the fractional change in the terminal slope (FCT) when tissues were progressively lumped from the longest transit time to shorter ones. This study was conducted to identify the practical threshold of K_{det} by applying the lumping theory to plasma/blood concentration-time relationships of 113 model compounds collected from the literature. We found that drugs having $K_{det} < 0.3$ were associated with $FCT < 0.1$ even when all peripheral tissues were lumped, resulting in comparable plasma concentration-time profiles between one-tissue minimal PBPK (mPBPK) and WB-PBPK models. For drugs with $K_{det} \geq 1$, WB-PBPK profiles appeared similar with two-tissue mPBPK models by applying the rule of $FCT < 0.1$ for lumping slowly equilibrating tissues. The two-tissue mPBPK model also appeared appropriate in terms of concentration-time profiles for drugs with $0.3 \leq K_{det} < 1$, although, some compounds (15.9% of the total cases), but not all, in this range showed a slight (maximum of 18.9% of the total AUC) deviation from WB-PBPK models, indicating that the two-tissue model, with caution, could still be used for those cases. Comparison of kinetic parameters between traditional (model-fitting) and current (theoretical calculation) mPBPK analyses revealed their significant correlations. Collectively, these observations suggest that the number of tissue groups could be determined based on the K_{det}/FCT criteria, and plasma concentration-time profiles from WB-PBPK could be calculated using equations significantly less complex.

Keywords Whole-body PBPK · Tissue lumping · Minimal PBPK · Number of tissue group · Bottom-up approach

Introduction

The most accessible tissue sampled in pharmacokinetic studies is blood/plasma. Those blood/plasma concentration-time data are typically analyzed using either (i) simple kinetic models, such as compartment models [1, 2] and minimal physiologically based pharmacokinetic (mPBPK) models [3], or (ii) more complex whole-body physiologically based pharmacokinetic (WB-PBPK) models [4]. One of the most notable differences between the two approaches would be the mathematical description of the blood/plasma pharmacokinetics, viz., bi-/tri-exponential functions for the simple models versus functions consisting of many exponential terms (e.g., 10 terms for a 9-tissue model) for WB-PBPK models [4]. Since the concentration-time profiles from experiments would graphically resemble the shape of only bi- or tri-exponential functions if drugs are given intravenously [5–7], some exponential terms in WB-PBPK models should be capable of being theoretically consolidated and simplified [8, 9] to mPBPK models [3], in light of the presence of similarity in kinetics of drug distribution to tissues. In our companion paper [10], we examined the theoretical basis for the consolidation and simplification of WB-PBPK to the minimal models. In particular, we found that drug-specific parameters, viz., tissue-to-plasma partition coefficient (K_p) and fractional distribution parameter (f_d) of multiple tissues

✉ Suk-Jae Chung
sukjae@snu.ac.kr

[1] College of Pharmacy and Research Institute of Pharmaceutical Sciences, Seoul National University, 1 Gwanak-ro, Gwanak-gu, Seoul 08826, Republic of Korea

in WB-PBPK could be symbolically consolidated into those parameters of the lumped tissue group (i.e., $K_{p,lum}$ and $f_{d,lum}$) by Eqs. 1a and 1b:

$$K_{p,lum} = \frac{\sum V_T K_p}{\sum V_T} \tag{1a}$$

$$f_{d,lum} = \frac{\sum Q_T f_d}{\sum Q_T} \tag{1b}$$

This principle implies the preservation of the total apparent volume of distribution and distributional clearance for the lumped tissue (i.e., $\sum V_T \cdot K_{p,lum}$ and $\sum Q_T \cdot f_{d,lum}$) from those tissues before lumping (i.e., $\sum V_T K_p$ and $\sum Q_T f_d$). We also proposed that the appropriateness of tissue lumping could be appraised by evaluating the impact of the lumping procedure (UET_{SEG}, a unitless error term for the construction of SEG) on the terminal phase slope (λ_{ter}), expressed as the fractional change in λ_{ter} (FCT) (Eq. 2) [10]:

$$FCT = \frac{\lambda_{ter}{}' - \lambda_{ter}}{\lambda_{ter}} \approx K_{det}{}^2 \cdot UET_{SEG} \tag{2}$$

We showed [10] that K_{det}, a drug-specific parameter and a determining coefficient for the number of tissue groups, could be calculated as the ratio of MTT_{max} (i.e., the maximum MTT value among tissues in WB-PBPK) to MRT_B (i.e., the mean residence time in the body).

In this study, we aimed to determine the threshold condition of K_{det} for the number of tissue groups when simplifying a WB-PBPK model to a mPBPK model based on the lumping theory proposed in our companion study [10]. We collected plasma/blood concentration-time data of 113 compounds after intravenous administration to rats from the literature and using in silico predictions based on a series of empirical correlations to calculate the K_p and f_d values of those model compounds. We report that the systemic pharmacokinetics of drugs having K_{det} less than 0.3 may be described by a one-tissue mPBPK model, while drugs having K_{det} greater than or equal to 0.3 may be practically described by a two-tissue mPBPK model.

Methods

Collection of Concentration-Time Data from the Literature

To study the adequacy of the theory of tissue lumping proposed in our companion paper [10], we collected the plasma/blood concentration-time information for 113 compounds after intravenous administration to rats from the literature (Supplementary Table SI). The model compounds encompassed 4 types of ionization (i.e., acid, base, neutral, and zwitterion). The 113 compounds have systemic clearance (CL_{sys}) values ranging from 0.0303 to 292 mL/min/kg and steady-state volume of distribution (V_{ss}) values ranging from 0.117 to 19.9 L/kg.

The concentration-time relationships from the literature were first digitized using GetData software (GetData Graph Digitizer version 2.26). Standard non-compartmental analyses, using WinNonlin Professional® 5.0.1 software (Pharsight Corporation, Mountain View, CA), were then conducted using the digitized data to calculate model-independent pharmacokinetic parameters. The digitization process used in this study was assumed to be adequate when the fold-difference of crucial parameters (e.g., V_{ss} and CL_{sys}) were within a factor of 1.5 between the literature value and the current calculation. The adequate datasets were then used for the subsequent pharmacokinetic calculations.

Estimation of Biopharmaceutical Variables of Model Compounds for Use in WB-PBPK Calculations

The physicochemical properties, including log P, log D, the number of hydrogen bond donor and acceptor (HD and HA; ACD/Labs Percepta Platform available from http://www.chemspider.com/), pKa [MarvinSketch™ software version 15.1.11.0 (http://www.chemaxon.com)], and topological polar surface area ($TPSA$; http://molinspiration.com/), of the 113 compounds were initially estimated from their chemical structure. To predict the free fraction in plasma (f_{up}) of the rat, the human f_{up} values were first calculated [11] by utilizing Simcyp® Version 15 Release 1 (Simcyp Limited, Sheffield, UK) [12]. The rat free fraction is assumed to be identical to the human value [13]. Similarly, human K_b [Eq. 3a; i.e., the ratio of the drug concentration in red blood cells to that in plasma water ($C_{rbc}/C_{u,plasma}$)] was assumed to be a reasonable estimate for rat values [14] and, thus, the blood-to-plasma partition coefficient (R) was calculated using the following equation (Eq. 3b) where Hct represents the hematocrit (i.e., 0.45) in rats:

$$\log K_b = 0.617 \cdot \log\left[\left(1 - f_{up}\right)/f_{up}\right] + 0.208 \tag{3a}$$

$$R = \left(K_b \cdot f_{up} - 1\right) \cdot Hct + 1 \tag{3b}$$

To estimate the parallel artificial membrane permeability assay (PAMPA) value ($P_{app,PAMPA}$) [15], the relationship (Eq. 4) between the permeability and physicochemical properties, such as log P, log D, pKa, molecular weight (MW), HD, HA, and $TPSA$ (Supplementary Table SII) was determined using a similar approach to a previous report [16]:

$$\log P_{app,PAMPA} = -10.1039 + 0.1663 \cdot \log P - 0.2158 \cdot |\log P - \log D| + 1.8332 \cdot \log MW + 0.3797HA + 0.0801HD^2 - 0.0453 \cdot TPSA \quad (4)$$

From this empirical relationship (Supplementary Fig. S1), $P_{app,PAMPA}$ values for the compounds were calculated and used for the estimation of f_d in 11 major tissues of rats, depending on the tissue distribution Models 1 and 2 [10, 17].

Assuming symmetrical transport rates into and out of tissues, K_p values for tissues were estimated in silico using the mechanistic prediction methods [18, 19] [i.e., Method 2 in the Simcyp® simulator [12]]. Then V_{ss} for the 113 compounds was then estimated using the following relationship (Eq. 5) [20]:

$$V_{ss} = V_p + V_{rbc} \cdot EP + \sum V_{T,i}K_{p,i} \quad (5)$$

where V_p and V_{rbc} are the volume of plasma and red blood cells; and EP is the erythrocyte-to-plasma partition coefficient (i.e., $K_b \cdot f_{up}$). For the elimination kinetics, CL_{sys}, obtained from non-compartmental analyses from the digitized data, was used in differential equations for the arterial blood (for Models A and B, Fig. 1) and the lumped blood pool (for Models C, D, and E, Fig. 1; see below for detailed descriptions of the model structures). The physiological variables, such as V_T and Q_T, required in PBPK calculations, were obtained from the literature [12, 21] and summarized in Table I. These values were essentially comparable to those used in the commercial software such as Simcyp® Version 15 Release 1. Numerical integration, using the fourth-order Runge-Kutta method, was carried out with Berkeley Madonna™ software (version 8.3.18; University of California, Berkeley, CA, USA). When needed, the calculation of eigenvalues and eigenvectors of PBPK system matrices was conducted using Python™ version 3.6.0. (www.python.org), based on the assumption of instantaneous drug distribution within the blood pool at time zero.

Table I Summary of Physiological Input Parameters Used in WB-PBPK Calculations in Rats for a Bottom-Up Approach of Tissue Lumping, Obtained from the Literature [12, 21]

	Tissue volume (mL)	Blood flow (mL/min)
Liver	8.57	19.4
Brain	1.24	1.12
Kidney	2.19	11.6
Heart	1.05	3.2
Lung	1.24	80
Spleen	0.57	0.88
Gut	6.19	8.08
Muscle	116	19
Adipose	16.7	4.72
Skin	39.4	4.08
Bone	15.7	8.08
Venous blood	10.2	
Arterial blood	5.11	

Tissue Lumping Process and Model Evaluation

Our strategy for tissue lumping in WB-PBPK model (Fig. 1a; Model A) could be summarized by 4 sequential steps: lumping of (i) the liver, gut, and spleen (i.e., splanchnic tissues) (Fig. 1b; Model B); (ii) the venous and arterial blood (i.e., the blood pool) (Fig. 1c; Model C, in a form of conventional multi-compartment mammillary model); (iii) the peripheral tissues segregated into SEG or REG using

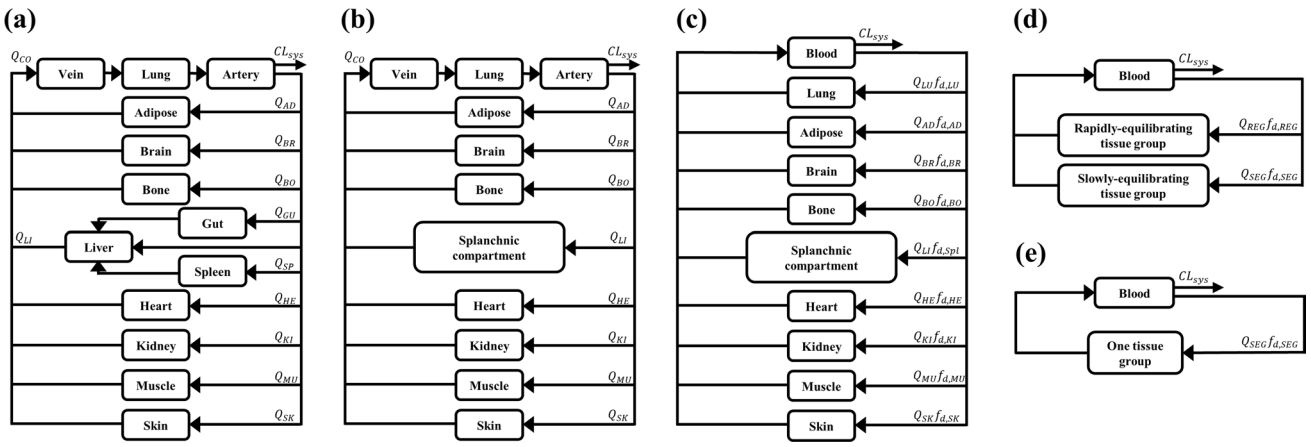

Fig. 1 Schematic representation of PBPK models considered in the tissue lumping procedure: WB-PBPK models **a** consisting of 11 tissues (viz., adipose, bone, brain, gut, heart, kidney, liver, lung, muscle, skin, and spleen) (Model A), **b** with a modification of Model A by lumping liver, gut, and spleen into a splanchnic compartment (Model B), **c** in a shape of mammillary compartment model with the splanchnic and blood pool compartments (Model C); and **d** two-tissue and **e** one-tissue mPBPK model structures (Models D and E)

Eqs. 1a, 1b, and 2 (Fig. 1d; Model D, model with two tissue groups); and (iv) all the peripheral tissues consolidated into a single distribution pool (Fig. 1e; Model E, model with one tissue group).

The adequacy of each step of lumping was evaluated for 113 model compounds by monitoring the following ancillary criteria: (i) the terminal phase slope (λ_{ter}); (ii) the area under the curve of the pharmacokinetic profiles from time 0 to t_{last} (AUC_{last}); and (iii) the root mean square of logarithmic difference (RMSLD) represented as:

$$RMSLD = \sqrt{\frac{\sum \left(\log C_{pred} - \log C_{obs}\right)^2}{n}} \tag{6}$$

where C_{pred} and C_{obs} are the predicted and observed plasma/blood concentrations and n is the number of observed points. When necessary, we also calculated the difference in model predictions using the following equation:

$$y = \frac{\int_0^{t_{last}} \left|\log_2\left(\frac{C_{lumped}}{C_{WB-PBPK}}\right)\right| dt}{t_{last}} \tag{7}$$

where $C_{WB-PBPK}$ and C_{lumped} are the results of model predictions from WB-PBPK and lumped models, and t_{last} is the last sampling time. With a dt value fixed to be 0.01 min in Eq. 7, the lumping process was assumed to be adequate when a fold-change of calculated criteria was within a factor of 2 between the simplified model and the WB-PBPK model. When necessary, the FCT [$(\lambda_{ter}{}' - \lambda_{ter})/\lambda_{ter}$, Eq. 2] and the ratio of slopes in the initial (λ_α/λ_1) and distributional ($\lambda_\beta/\lambda_{major}$) phases [10] were also monitored to determine the appropriateness of segregating peripheral tissues into SEG and REG in Model D. In addition, a unitless error term for the construction of REG, UET_{REG}, was calculated to determine the adequacy of lumping of tissues into the REG as shown in our companion paper [10].

In this study, we were also interested in determining the appropriateness of the SEG construction based on the fold-difference in MTT values [22] as an ancillary method. Thus, a sequential lumping, based on Eqs. 1a and 1b, in the direction from the tissue having the longest MTT (MTT_{max}) to tissue(s) having the shorter MTT(s) was carried out. In addition, the similarity condition of MTT (viz., MTT values that were considered kinetically "equivalent") was investigated for various cases of each model compound. The three validation criteria (RMSLD, λ_{ter}, and AUC_{last}); calculated from 1808 simulations after lumping [i.e., 113 compounds × 2 models (Models 1 and 2) × 8 combinations (with 9 peripheral tissues)]; were compared with those from Model C (before lumping), depending on the ratio of the maximum to the minimum MTT (MTT_{max}/MTT_{min}) for the tissues included in SEG. In this process, the model predictions were also assumed to be indistinguishable when a fold-change of the criteria between the models fell within a factor of 2.

Determination of Threshold Value of K_{det} for Use of One-Tissue mPBPK

In this study, we determined the threshold condition between models having one tissue group and two tissue groups. As proposed in our companion paper [10], K_{det} was regarded as a key determinant here. When necessary, we also considered the area ratio of S_{rec} (i.e., area representing the distributional phase in rectangular coordinates, determined by three exponential curves from Model D) to AUC (i.e., area under the curve from time 0 to infinity) as a criterion of the kinetic contribution of the distributional phase to the shape of a comprehensive pharmacokinetic profile [10]. In Model D (i.e., $C_p(t) = C_\alpha e^{-\lambda_\alpha t} + C_\beta e^{-\lambda_\beta t} + C_\gamma e^{-\lambda_\gamma t}$, under the condition $\lambda_\alpha > \lambda_\beta > \lambda_\gamma$), S_{rec} could be calculated using the log-trapezoidal method (Eqs. 8a and b):

$$AUC_{t_i-t_j} = \frac{C_p(t_i) - C_p(t_j)}{\ln\left(C_p(t_i)\right) - \ln\left(C_p(t_j)\right)}\left(t_j - t_i\right) \quad (i,j = 1,2,3 \text{ and } i \neq j) \tag{8a}$$

$$S_{rec} = AUC_{t_1-t_3} - AUC_{t_1-t_2} - AUC_{t_2-t_3} \quad (\text{for } t > 0) \tag{8b}$$

where three points $T_1{}'(t_1, C_p(t_1))$, $T_2{}'(t_2, C_p(t_2))$, and $T_3{}'(t_3, C_p(t_3))$ represented the intersection points determined by each pair of $C_\alpha e^{-\lambda_\alpha t}$ and $C_\beta e^{-\lambda_\beta t}$, $C_\alpha e^{-\lambda_\alpha t}$ and $C_\gamma e^{-\lambda_\gamma t}$, and $C_\beta e^{-\lambda_\beta t}$ and $C_\gamma e^{-\lambda_\gamma t}$. Using the similar principles to determine S_{log} [10], we examined the change in S_{rec}/AUC depending on K_{det} for the 113 model compounds. If the contribution of S_{rec} to AUC is sufficiently small under a certain range of K_{det}, Model D structures would essentially become consistent with Model E structures.

Reconciliation of mPBPK Models Between Bottom-Up and Top-Down Approaches

The simplified models used in this study, Models D and E, were virtually identical to mPBPK structures, except their kinetic parameters were determined by fitting (i.e., traditional mPBPK analyses) or calculation (i.e., the current approach). Based on the lumping criteria proposed in this study (see the "Results" section), the current models (Model D/E) could be written in the format of these mPBPK models (Eqs. 9a and 9b) [3]:

$$V_B R \frac{dC_p}{dt} = Dose\ rate - \sum_{i=1}^{m} Q_{T,lum,i} f_{d,lum,i} R \cdot \left(C_p - \frac{C_{T,lum,i}}{K_{p,lum,i}}\right) - CL_{sys} C_p \tag{9a}$$

$$V_{T,lum,i}\frac{dC_{T,lum,i}}{dt} = Q_{T,lum,i}\,f_{d,lum,i}R\cdot\left(C_p - \frac{C_{T,lum,i}}{K_{p,lum,i}}\right) \quad (i = 1 \text{ or } 2) \tag{9b}$$

For theoretical calculations of $K_{p,lum}$ and $f_{d,lum}$ (i.e., bottom-up), Eqs. 1a and 1b were applied using in silico predictions of K_p [18, 19] and model-dependent calculations of f_d [17] for rat tissues in WB-PBPK.

To validate the current "bottom-up" approach of tissue lumping, the kinetic parameters from a series of in silico predictions were compared with those determined by the model fitting methods (i.e., top-down) in two ways. First, 101 equally spaced concentration-time points from time 0 to 5 times the terminal phase half-life were theoretically generated using the analytical solution of Model C (i.e., a 10-exponential function for bolus injection) for the 113 model compounds. The number of tissue groups was determined using K_{det} and the errorless datasets subjected to nonlinear regression analysis based on Eqs. 9a and 9b depending on their mPBPK models. Second, the experimental data for the 113 compounds were prescreened for which (i) the *in silico* prediction of V_{ss} was within a factor of 2 and (ii) the terminal phase in the simulated profile was apparently reached at the last sampling time observed in the literature. Based on the above screening method, 31 compounds were selected and their experimental concentration-time data fitted to the appropriate mPBPK models (Eqs. 9a and 9b). When fitting the errorless and experimental datasets to Eqs. 9a and 9b to determine $f_{d,lum}$ values (i.e., top-down), the calculated $K_{p,lum}$ from Eq. 1a was used. The resulting top-down $f_{d,lum}$ values were then compared with the bottom-up $f_{d,lum}$ values (Eq. 1b). In addition, the three ancillary criteria (λ_{ter}, AUC_{last}, and RMSLD) were also compared between bottom-up and top-down approaches of mPBPK models.

Results

Calculation of Biopharmaceutical Variables for Model Compounds

The K_p values for 113 model compounds in 11 typical tissues of WB-PBPK were calculated using their estimated f_{up}, R, log P, and pKa values [18, 19] (see Supplementary Material 1 for the preliminary calculation results). To examine the validity of in silico determined K_p values used in this study, V_{ss} values for the 113 model compounds were then estimated using Eq. 5. Despite assuming a lack of species difference in blood partitioning between humans and rats (i.e., f_{up} and R), V_{ss} estimated from the predicted K_p values ($V_{ss,pred}$) was significantly correlated with V_{ss} calculated from standard moment analyses for the blood/plasma pharmacokinetics ($V_{ss,obs}$) of the model compounds (Supplementary Fig. S2) (i.e., $\log V_{ss,obs} = 0.972+0.695\cdot\log V_{ss,pred}$, n = 113, R^2 = 0.479; Pearson's test for correlation, $p < 0.001$). We found that the number of V_{ss} values within factors of 2 and 3 were 59 and 85 out of 113 compounds (52.2% and 75.2%).

In this study, we also determined the validity of in silico predictions for f_d values depending on distribution Models 1 and 2. Since the inclusion of f_d in WB-PBPK calculations improved the predictability of systemic pharmacokinetics [17], RMSLD (a predictability criterion) calculated using Model A was also evaluated. The number of compounds with RMSLD less than 0.301 and 0.477 (i.e., predictability within a factor of 2 and 3) was 39 and 68 (34.5% and 60.2%) for Model 1, and 43 and 73 (38.1% and 64.6%) for Model 2. Collectively, therefore, it was assumed that K_p and f_d values generated by the current methods were practically useful, since the results was fairly reasonable with existing values of K_p [18, 19] and f_d [17]. The computational K_p and f_d values for the 113 model compounds were then used in subsequent calculations for blood/plasma pharmacokinetic profiles. We noted that some model compounds had relatively poor predictability for K_p and f_d, thereby affecting the calculation of concentration-time relationship. However, the primary objective of this study was to compare theoretical pharmacokinetic profiles from Model C to those from Model D/E, rather than to compare actual experimental concentration-time data with model predictions. Therefore, we were more focused on generating a realistic range of physicochemical/biopharmaceutical parameters for the calculations. Those compounds associated with poor predictability for K_p and f_d were, therefore, also included in pharmacokinetic calculations. In the real application of the current theoretical approach, experimentally determined K_p and f_d values for each compound would have been used resulting in more reasonable prediction of the concentration-time profiles of the compound.

Impact of Tissue Lumping on Shape of Concentration-Time Relationships

Lumping of Splanchnic Tissues

We found that the splanchnic tissues (liver, gut, and spleen) may be mathematically combined, as shown in our companion paper [10], as if they were connected in parallel to the systemic circulation system (e.g., vein and artery). Applying our tissue lumping principle [10], it was evident that in drugs with perfusion-limited distribution to the liver (i.e., $f_{d,LI} \rightarrow 1$), distribution in the other splanchnic tissues (e.g., spleen and gut) would have negligible effects to the distribution kinetics to the splanchnic compartment. At the other extreme, when the apparent PAMPA permeability coefficient was sufficiently small (i.e., $f_{up}P/R < 1\times10^{-6}$ cm/s) [17], for the example when K_p values are comparable between the liver, gut, and spleen (Supplementary Fig. S3), reciprocal

MTT values for the modified tissues (i.e., $1/MTT_{SP}{}'$ and $1/MTT_{GU}{}'$, both corrected by $1-f_{d,LI}$) [10] would be comparable to $1/MTT_{LI}$, regardless of the tissue distribution Models 1 and 2. Even when K_p values for liver, gut, and spleen were significantly different from each other, a significant model deformation with respect to the plasma pharmacokinetics did not appear to occur (Supplementary Material 2; the analytical solutions indistinguishable between Models A and B), since the coefficients for the zero- and first-order expansion terms of fractions in the left-hand sides between Eqs. 11 and 12 (see Appendix A) were retained in most of the tissues including liver, gut, and spleen (i.e., conservation of $\sum V_T K_p$ and $\sum Q_T f_d$) [10]. Thus, we found that these tissues could be practically lumped into the splanchnic compartment without causing a significant deviation in the calculation of the concentration-time relationship of Model B from Model A.

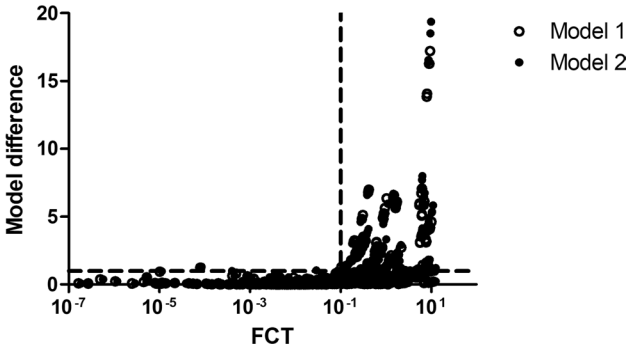

Fig. 2 Discrimination of peripheral tissues into SEG or REG by utilizing *FCT* as an index of tissue lumping. Segregation of tissues into SEG or REG was carried out by monitoring *FCT* from various lumping cases generated for the 113 model compounds. Model difference (y-axis) was calculated as Eq. 7, and horizontal dashed line denoted the fold-difference in model predictions with a factor of 2

Lumping of Blood Pool

After constructing the splanchnic compartment, we then attempted to combine venous and arterial blood into a single blood pool. Calculated parameters, such as RMSLD, λ_{ter}, and AUC_{last} values (Supplementary Fig. S4), generated using the original Model A and the Model B with combined venous/arterial blood (i.e., Model C) revealed that the predictions were quite comparable between those models. As also shown in Supplementary Material 2, this observation indicates that the lumping of the venous and arterial blood into a single blood pool does not cause a significant deviation in the calculation of the concentration-time relationship except for the difference in the initial concentration (i.e., $C_0=0$ for Model B; $C_0\neq 0$ for Model C). In line with this, we also considered consolidating the blood pool and lung into a single "systemic circulation" group (i.e., vein-lung-artery connection) by assessing how the inclusion of the lung in the blood pool impacted the calculation of the concentration-time relationship. While the lumping of lung into the blood pool would, in theory [23], affect all eigenvalues of the solution of Model C, it was found that the initial phase slope λ_1 was mostly altered by a fold-change in MTT_c (i.e., mean transit time through the central compartment) (Supplementary Fig. S5). Considering the alteration of λ_1 by lumping of lung into the blood pool, therefore, we ultimately chose to utilize Model C, i.e., the blood pool consisting of arterial and venous blood while the lung was regarded as one of the peripheral tissues, as the reference model to compare with simplified model structures.

Lumping of SEG

In order to determine appropriate criteria for tissue lumping, we considered segregating peripheral tissues into SEG or REG according to *FCT*. We used *FCT* as a determinant because the fractional change was a function of both the compound-specific K_{det} and the lumping-dependent UET_{SEG} (Eq. 2). Our premise was that peripheral tissues could be progressively lumped into the SEG from the tissue having the longest *MTT* to tissue(s) having shorter *MTT*(s) provided that λ_{ter} does not change significantly. If the change in λ_{ter} exceeded a certain threshold *FCT* value, then further lumping of tissues into the SEG ceased and the remaining peripheral tissues could then be collectively lumped into the REG. As shown in Fig. 2, SEG/REG construction with the value of *FCT* up to 0.1 resulted in comparable concentration-time relationships calculated from Model C (without lumping of peripheral tissues) and those from Model D or E (with lumping of peripheral tissues to SEG/REG) within a factor of two (Eq. 7). Therefore, it was proposed that the condition of *FCT* at 0.1 was a reasonable threshold for SEG construction.

Determination of the Number of Tissue Groups in Simplified PBPK Model Using K_{det}

Since K_{det}, the determining coefficient for the number of tissue groups, has not been defined in current literature, the parameter was initially calculated for two compounds (e.g., caffeine and cefazolin) to show how K_{det} could play a role in the lumping of peripheral tissues. As shown in Fig. 3a, when a drug had a very low value of K_{det} (e.g., 0.0185 for caffeine), λ_{ter} did not change significantly even when UET_{SEG} value varied up to 15. In contrast, the λ_{ter} of cefazolin with a K_{det} value of approximately 4.97 was quite sensitive to changes to UET_{SEG}. This indicated that a drug with a low K_{det} value would have a robust λ_{ter} which is less sensitive to the change in UET_{SEG}, a parameter that was governed by the lumping of the slow tissue group. The systemic

(a)

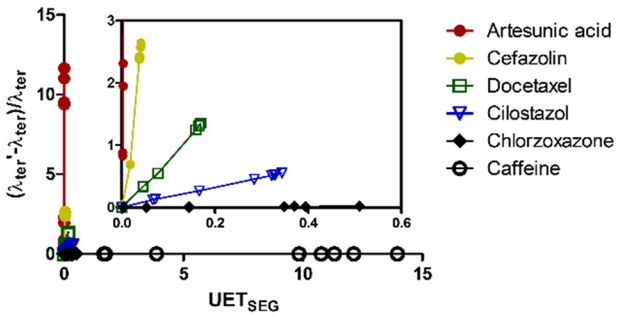

Compounds	K_{det}
Artesunic acid	55.4
Cefazolin	4.97
Docetaxel	2.28
Cilostazol	1.12
Chlorzoxazone	0.183
Caffeine	0.0185

(b)

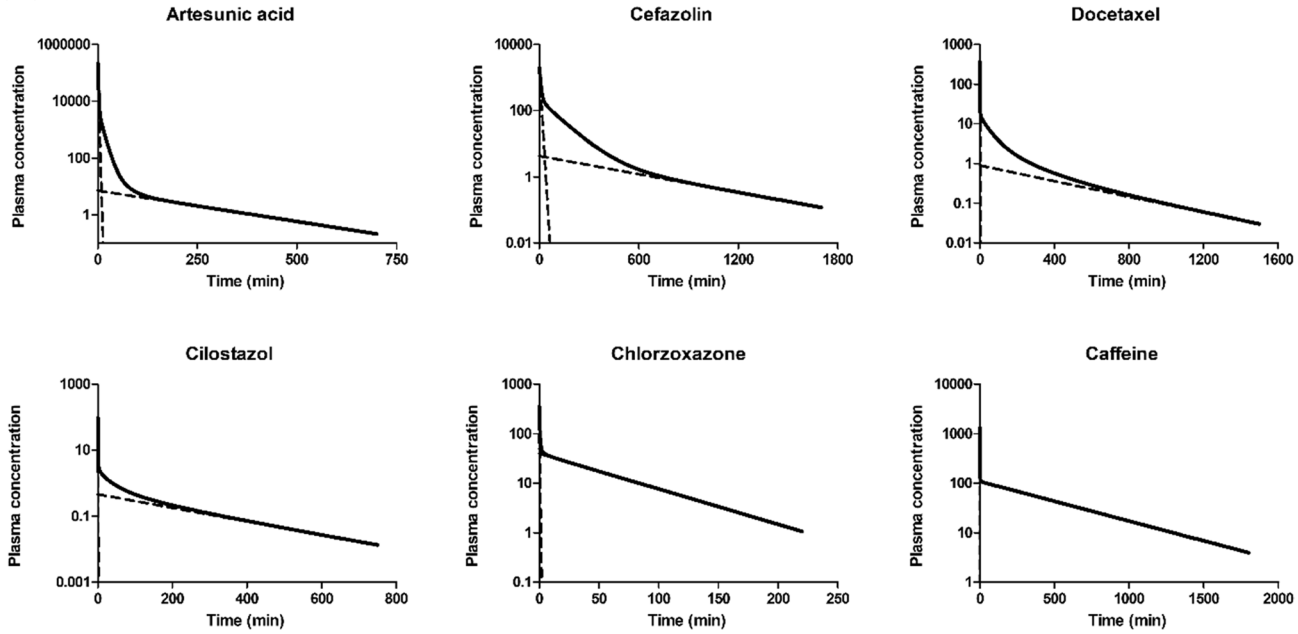

Fig. 3 **a** Sensitivity of the terminal phase slope expressed as *FCT* $[(\lambda_{ter}{}' - \lambda_{ter})/\lambda_{ter}]$ to the effect of SEG construction (UET_{SEG}) (i.e., $K_{det}{}^2$ to be the apparent slope of the plot). Six example compounds for a range of K_{det} values were included (e.g., artesunic acid, cefazolin, docetaxel, cilostazol, chlorzoxazone, caffeine). **b** Graphical presentation of the contribution of distributional area (S_{rec}) to *AUC*, depending on K_{det}. Solid lines denote the systemic pharmacokinetics of the 6 compounds Model C, while dashed lines represent the terminal ($C_{10}e^{-\lambda_{10}t}$) or initial exponential term ($C_1e^{-\lambda_1 t}$). The plasma concentrations were calculated up to the time at 5-fold of the terminal phase half-life ($5\ln 2/\lambda_{10}$)

pharmacokinetics of 4 additional compounds: artesunic acid, chlorzoxazone, cilostazol, and docetaxel in Model C (with regard to tissue distribution Model 1) were also shown in Fig. 3b. The data in Fig. 3b for these 6 compounds suggest that, when K_{det} is sufficiently low, the contribution of the distributional area S_{rec} to the total *AUC* becomes kinetically insignificant so that all peripheral tissues could be combined (Model E). Therefore, we aimed to determine the number of tissue groups in the simplified PBPK model (Models D and E) based on K_{det}.

When all the nine peripheral tissues were deliberately lumped into one tissue group (Model E), the data for the 113 model compounds showed noticeable monotonic increase in *FCT* values along with their K_{det} values (Fig. 4a) (e.g., an empirical correlation between *FCT* and K_{det} up to the K_{det} range of 10, $\log FCT = -0.433 + 1.14 \cdot \log K_{det}$, $R^2 = 0.946$). However, the apparent linear relationship between *FCT* and K_{det} slightly deviated for model compounds with K_{det} values larger than 10. When we considered a threshold condition of $K_{det} < 0.3$, all the compounds satisfying this condition [i.e., 29 cases, ~12.8% of the total 226 cases (113 compounds in two distribution models)] showed *FCT* values less than 0.1, suggesting that the change in λ_{ter} remains insensitive even when all the peripheral tissues were lumped into one tissue group (i.e., Fig. 4a). Of note, 6 exceptions (cisplatin and indomethacin for Model 1; acyclovir, cisplatin,

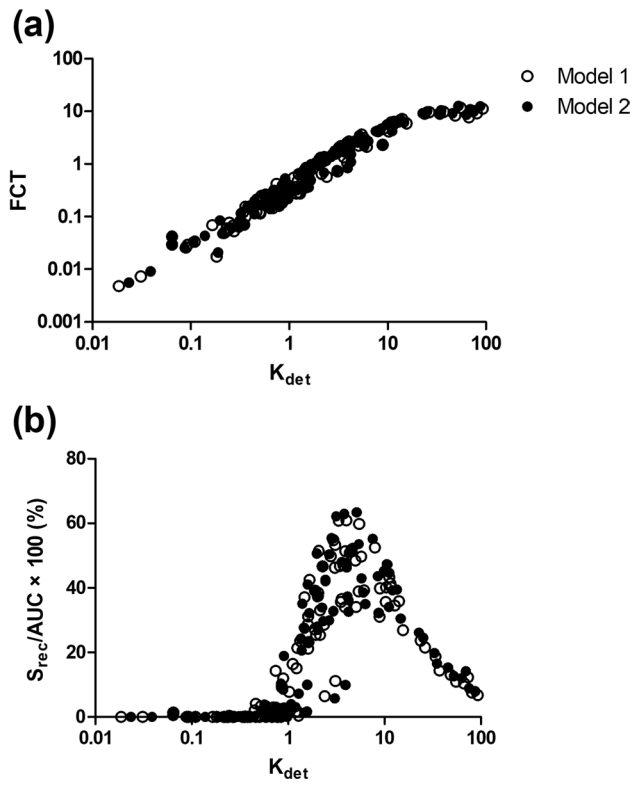

Fig. 4 Impact of K_{det} for 113 model compounds on **a** the *FCT* assuming one-tissue mPBPK and **b** the change in S_{rec}/AUC ratio assuming two-tissue mPBPK. $K_{det} < 0.3$ resulted in the robust terminal phase ($FCT < 0.1$) and the S_{rec}/AUC ratio approximately less than 2% showing the adequate use of one-tissue mPBPK (Model E). Open and closed circles denote simulation results from the tissue distribution Models 1 and 2

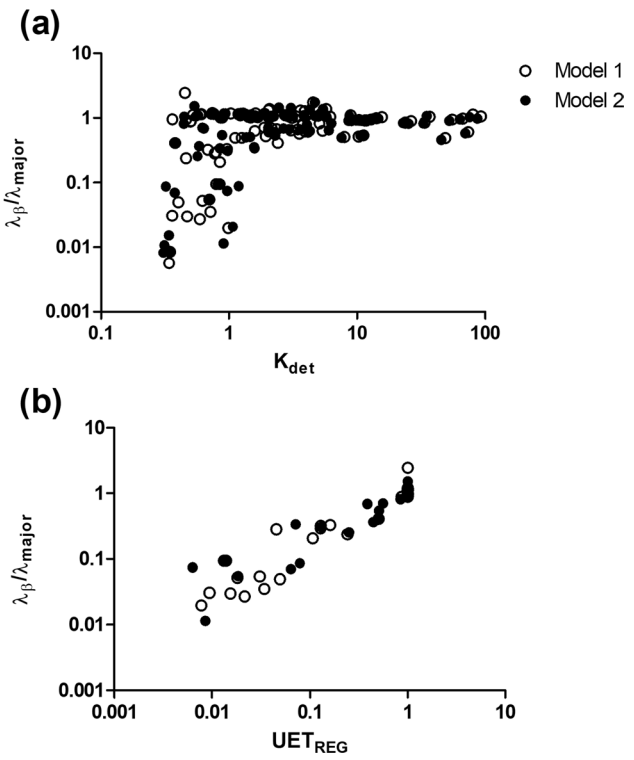

Fig. 5 Comparison between the distributional phase slope of Model D (λ_β) and Model C (λ_{major}) as the ratio of $\lambda_\beta/\lambda_{major}$, **a** depending on K_{det}, and **b** predicted by UET_{REG} for the K_{det} range between 0.3 and 1, after segregation of 9 peripheral tissues into SEG or REG based on the condition of $FCT < 0.1$

erythromycin, and terazosin for Model 2) with K_{det} ranging from 0.308 to 0.350 also exhibited *FCT* less than 0.1. Collectively, this monotonic increase was consistent with the statement that a drug with a low K_{det} value, e.g., below 0.3, would have a robust λ_{ter} so that all peripheral tissues could be lumped into one tissue group.

On the other end, we also aimed to monitor the contribution of the speculative area, S_{rec}, to *AUC* depending on K_{det} for all 113 model compounds. For the purpose of this calculation, we intentionally divided peripheral tissues into two groups (i.e., two-tissue mPBPK models). To construct Model D from Model C using a method independent of K_{det} values, we considered applying an alternative method for the construction of the SEG (i.e., peripheral tissues lumped into an SEG according to the rule of $MTT_{max}/MTT_{min} < 2$; Supplementary Fig. S6) [22]. When the S_{rec}/AUC ratio (Eq. 8b) was plotted against K_{det} (Fig. 4b), the kinetic contribution appeared to be negligible when $K_{det} < 0.3$ (e.g., $S_{rec}/AUC < 1.35\%$; for colistin sulfate), supporting the adequacy of Model E in the range. We observed that some compounds with K_{det} sufficiently larger than 5 (Fig. 4b) could be associated with a low S_{rec}/AUC ratio; this characteristic may not be interpreted as the evidence that an appropriate model for those compounds would be Model E (i.e., bi-exponential relationship) since a large value of K_{det}, e.g., larger than 5, would indicate that any lumping of peripheral tissues drastically altered λ_{ter} (Fig. 3a). Therefore, even with low S_{rec}/AUC ratios, the systemic pharmacokinetics was more likely to be described by Model D for compounds with such high K_{det} values.

Consideration for Lumping of REG

For compounds having $K_{det} \geq 0.3$, *FCT* was not likely to be sufficiently robust since, at a certain point of tissue lumping, the terminal phase could be drastically affected. Thus, the construction of the REG became necessary. Initially, we found that the model predictions of Model D (i.e., blood pool plus 2 tissue groups with different equilibrating rates) and that of Model C (i.e., blood pool plus nine peripheral tissues) were almost always within a factor of two where *FCT* of 0.1 was used as the threshold (Fig. 2). To further determine the

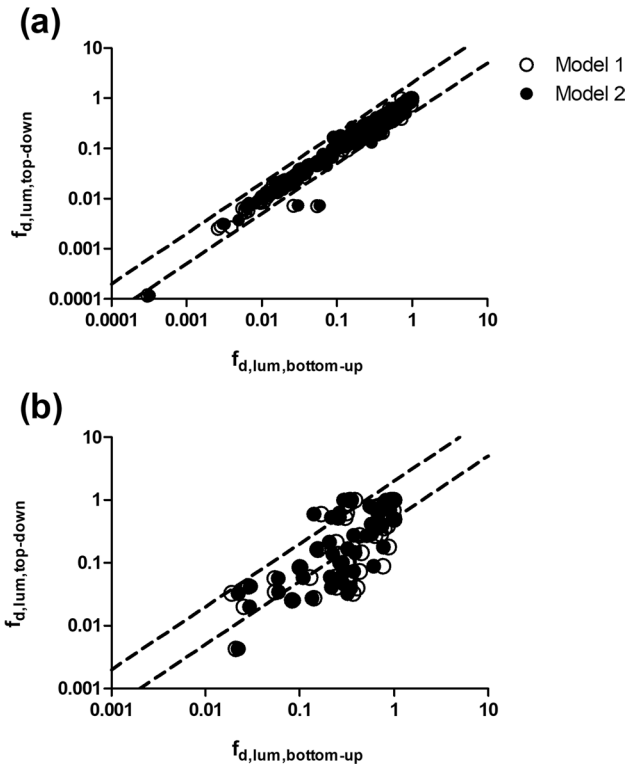

Fig. 6 Relationship between the fractional distributional parameters, $f_{d,lum}$, calculated by bottom-up and top-down approaches in mPBPK models. The $f_{d,lum}$ values calculated from bottom-up approach was plotted against top-down values fitted to: **a** the errorless data from Model C for 113 model compounds and **b** the experimental observations for a subset of 31 compounds. Dashed lines represented the two-fold difference between top-down and bottom-up approaches for the parameters. Open and closed circles denoted calculation results from Models 1 and 2

adequacy of REG construction with this principle, we evaluated whether λ_β in Model D was comparable with λ_{major} in Model C [10] using the 113 model compounds. As shown in Fig. 5a, it was readily evident that λ_β was comparable to λ_{major} for most compounds having $K_{det} > 1$, indicating that *FCT* of 0.1 was a reasonable threshold for the segregation of SEG and REG for those compounds.

However, for the compounds having $0.3 \le K_{det} < 1$ [i.e., 63 cases; 27.9% of the total of 226 (113 compounds in two distribution models)] some, but not all, compounds had a significant dissociation between λ_β and λ_{major} (i.e., 36 cases; 15.9% of the total) (Fig. 5a). Since some compounds in this range still had comparable λ_β and λ_{major} values, the rule of *FCT* at 0.1 remains applicable when determining the appropriateness of the lumping of tissues. Even for those compounds having a significant difference between λ_β and λ_{major} values, however, the calculation results between Models C and D remained fairly accurate (Fig. 2). Furthermore, the contribution of S_{rec} to the total *AUC* was only approximately 18.9% (i.e., Model 1 for tamoxifen; Fig. 4b) or less for those compounds, suggesting that its effects on the plasma concentration-time relationship is potentially minor. Therefore, for the sake of practicality we cautiously recommend to apply the threshold of *FCT* at 0.1 for the SEG construction even for those compounds in the range $0.3 \le K_{det} < 1$, while the other remaining peripheral tissues can then be collectively lumped as the REG.

Reconciliation of mPBPK Models Between Bottom-Up and Top-Down Approaches

If the theoretical consideration was adequate, a statistically acceptable correlation would be found between calculated vs. fitted parameters (i.e., bottom-up vs. top-down) for a given set of compounds. Here, such a reconciliatory study was first carried out using PBPK calculations for the 113 model compounds. When the errorless simulation data (i.e., 101 points generated from a 10-exponential function for Model C) were fitted to the mPBPK model structures (Model D for $K_{det} \ge 0.3$ and Model E for $K_{det} < 0.3$), these top-down $f_{d,lum}$ values were consistent with bottom-up $f_{d,lum}$ values (Fig. 6a; see Supplementary Table SIII for details). In this correlation, a few points did not fall within a factor of 2, which were the cases with K_{det} values (for Models 1 and 2) between 0.3 and 1 [e.g., indomethacin (0.339 and 0.322) and ochratoxin (0.402 and 0.376)] or less than 0.3 [e.g., tolbutamide (0.0891 and 0.0863)]. Even for those 3 cases, however, RMSLD was found to be less than 0.0577, indicating that concentration-time profiles generated by bottom-up model predictions were fairly consistent with the corresponding datasets. For 31 compounds with experimental data (Table II), bottom-up $f_{d,lum}$ values were significantly correlated with top-down $f_{d,lum}$ values (Fig. 6b), based on the Pearson's correlation test (i.e., $R^2 = 0.367$ and 0.379 for Models 1 and 2; $p < 0.0001$ for both cases). The number of $f_{d,lum}$ values within factors of 2 and 3 were 50 and 68 out of 100 points, while the three criteria (RMSLD, λ_{ter}, and AUC_{last}) were comparable between the two approaches (Supplementary Fig. S7). Collectively, model predictions from the current bottom-up method appeared comparable with those from the top-down approach for the 113 model compounds.

Discussion

Systemic pharmacokinetics is a manifestation of the intricate operations of drug disposition kinetics (viz., WB-PBPK model) occurring within the body. Despite the theoretical complexity, however, plasma concentration-time data typically follow relatively simple bi- or tri-exponential decay

Table II Compound-Specific Input Parameters for the Reconciliation Study Between Bottom-Up and Top-Down Approaches Where the Experimental Data Were Utilized for Model Fitting of mPBPK Structures. The Symbols Represent Adipose (AD), Bone (BO), Brain (BR), Heart (HE), Kidney (KI), Lung (LU), Muscle (MU), Skin (SK), and the Splanchnic Compartment (SPL) of Rats (with 250 g Body Weight). Tissues Are Arranged in Ascending Order of *MTT* Values, Assuming That Tissue Constituents in REG and SEG Were Consistent Between Models 1 and 2

	K_{det}		REG ($i=1$)	SEG ($i=2$)	$K_{p,lum1}$	$K_{p,lum2}$	Bottom-up Model 1		Bottom-up Model 2		Top-down (CV%)	
	Model 1	Model 2					$f_{d,lum1}$	$f_{d,lum2}$	$f_{d,lum1}$	$f_{d,lum2}$	$f_{d,lum1}$	$f_{d,lum2}$
Caffeine	0.0185	0.0234	KI, LU, HE, AD, SPL, BO, BR, MU, SK	-	-	0.596	-	0.407	-	0.348	-	0.0401 (53.9)
Astragaloside IV	0.0643	0.0643	LU, KI, HE, AD, SPL, BR, BO, MU, SK	-	-	0.589	-	1	-	0.991	-	1 (56.6)
Tolbutamide	0.0891	0.0863	KI, SPL, HE, MU, LU, AD, BR, BO, SK	-	-	0.123	-	0.0546	-	0.0591	-	0.0564 (39.5)
Adriamycin	0.0931	0.105	KI, HE, LU, SPL, MU, BO, AD, BR, SK	-	-	0.504	-	0.256	-	0.224	-	0.138 (16.5)
Dapagliflozin	0.110	0.139	KI, LU, HE, SPL, BO, BR, MU, AD, SK	-	-	0.750	-	0.433	-	0.371	-	0.273 (339)
Cyclosporine	0.165	0.197	KI, HE, LU, SPL, MU, BO, BR, AD, SK	-	-	6.10	-	0.321	-	0.276	-	0.0613 (17.0)
Chlorzoxazone	0.183	0.189	KI, HE, LU, SPL, SK, MU, BO, AD, BR	-	-	0.468	-	0.240	-	0.212	-	0.0592 (88.5)
DA7867	0.215	0.209	KI, HE, LU, SPL, MU, AD, BO, BR, SK	-	-	0.518	-	0.0552	-	0.0597	-	0.0346 (45.2)
Etoposide	0.220	0.266	KI, HE, LU, SPL, AD, BO, MU, BR, SK	-	-	0.505	-	0.335	-	0.287	-	0.0474 (17.7)
Erythromycin	0.245	0.311	KI, LU, HE, AD, SPL, BO, BR, MU, SK	-	-	1.59	-	0.434	-	0.372	-	0.0733 (18.0)
Terazosin	0.267	0.338	HE, LU, KI, AD, BO, BR, SPL, MU, SK	-	-	3.08	-	0.451	-	0.387	-	0.145 (48.7)
Acyclovir	0.274	0.308	KI, HE, LU, AD, SPL, BO, MU, BR, SK	-	-	0.642	-	0.246	-	0.216	-	0.0408 (19.0)
PEITC	0.359	0.445	KI, HE, LU, SPL, BO, MU	BR, AD, SK	2.48	11.2	0.347	0.682	0.299	0.550	0.998 (187)	0.799 (54.4)
Colistin methanesulphonate	0.380	0.380	LU, KI	HE, BR, SPL, BO, AD, MU, SK	0.249	0.166	1	1	1	1	1 (fixed)	0.489 (38.2)
Clindamycin	0.452	0.535	LU, KI, HE, AD, BO	SPL, BR, MU, SK	0.890	1.76	0.340	0.986	0.291	0.905	0.999 (149)	0.697 (61.8)
Sildenafil	0.463	0.584	HE, KI	LU, SPL, AD, BO, BR, MU, SK	0.512	0.542	0.718	0.369	0.573	0.320	0.412 (322)	0.0328 (17.6)
Irinotecan	0.498	0.621	KI, HE, LU	AD, SPL, BO, BR, MU, SK	2.91	1.81	0.128	0.793	0.109	0.679	0.0588 (26.3)	0.597 (5.14)
Moxifloxacin	0.506	0.638	KI	HE, LU, AD, BO, SPL, BR, MU, SK	4.16	1.58	0.725	0.374	0.578	0.323	0.285 (114)	0.168 (25.0)
Morphine	0.591	0.750	KI, LU, HE, AD, SPL	BO, BR, MU, SK	0.895	1.40	0.317	0.878	0.266	0.772	0.100 (247)	0.179 (36.2)
Mirodenafil	0.591	0.723	KI, HE, LU, SPL, BO, MU	AD, BR, SK	0.534	1.11	0.328	0.628	0.283	0.513	0.103 (22.6)	0.271 (19.3)
Atenolol	0.761	0.938	KI, AD, LU, HE, SPL	BO, BR, MU, SK	0.945	1.58	0.244	0.789	0.207	0.680	0.213 (163)	0.358 (41.4)
Verapamil	0.773	0.970	HE, KI, LU, BO	BR, SPL, AD, MU, SK	3.61	4.19	0.169	0.862	0.142	0.743	0.599 (36.3)	0.388 (18.8)
Azosemide	0.861	0.850	KI, SPL, HE, LU, MU, AD, BR, BO	SK	0.0903	0.292	0.0839	0.101	0.0861	0.103	0.0253 (39.2)	0.0842 (50.2)
Methylphenidate	1.19	1.50	HE, KI, LU, AD, BO, SPL	BR, MU, SK	3.34	3.32	0.304	0.929	0.255	0.822	0.522 (19.9)	0.999 (28.5)
Propranolol	1.24	1.57	HE, KI, LU, AD, BO, BR, SPL	MU, SK	4.09	3.93	0.316	0.966	0.264	0.859	0.618 (45.1)	1 (44.0)
Methamphetamine	1.28	1.58	HE, KI, AD, LU, BO, SPL	BR, MU, SK	3.51	3.45	0.256	0.899	0.218	0.777	0.526 (22.4)	0.909 (30.3)
Methotrexate	1.60	1.65	KI, HE, SPL, LU, AD, MU, BO	BR, SK	0.243	0.421	0.142	0.156	0.135	0.151	0.0275 (22.4)	0.164 (97.2)

Table II (continued)

	K_{det}		REG ($i = 1$)	SEG ($i = 2$)	$K_{p,lum1}$	$K_{p,lum2}$	Bottom-up Model 1		Bottom-up Model 2		Top-down (CV%)	
	Model 1	Model 2					$f_{d,lum1}$	$f_{d,lum2}$	$f_{d,lum1}$	$f_{d,lum2}$	$f_{d,lum1}$	$f_{d,lum2}$
Dihydroartemisinin	1.60	2.01	KI, HE, LU, SPL, BO, MU, BR, AD	SK	1.91	5.41	0.388	0.768	0.333	0.610	1 (152)	0.0885 (31.3)
Epigallocatechin-3-gallate	1.89	2.01	LU, KI, HE, SPL, BO, BR, MU	AD, SK	1.53	7.10	0.624	1	0.577	0.948	0.759 (55.0)	0.999 (107)
Bumetanide	11.8	11.2	KI, SPL, HE, MU, LU, AD, BR, BO	SK	0.0843	0.288	0.0255	0.0285	0.0294	0.0301	0.0201 (18.5)	0.0426 (19.6)
DA6034	12.8	12.1	KI, SPL, HE, LU, MU, AD, BO, BR	SK	0.109	0.308	0.0190	0.0211	0.0223	0.0223	0.0327 (13.3)	0.00427 (7.9)

functions [5–7] when drugs are given intravenously. As a result, simplified models (e.g., mPBPK and compartment models) were often sufficient for the descriptive analyses of plasma pharmacokinetics. Rationalization for the dissociation between the theoretical complexity in PBPK models and the relative simplicity in actual data has not been clearly delineated in the literature. Theoretical bases for the simplification of WB-PBPK models may ultimately provide the predictive capability of the intuitive calculations of kinetic parameters in the simplified models.

In this study, we found that the concentration-time relationship could be practically calculated by Model D, for the purpose of comparing the initial, distributive, and terminal phase slopes. In particular, we considered the version of Model D that assumes the blood pool and lung are combined [$C_p(t) = C_\alpha{}' e^{-\lambda_\alpha{}' t} + C_\beta{}' e^{-\lambda_\beta{}' t} + C_\gamma{}' e^{-\lambda_\gamma{}' t}$] and the version of Model D that assumes separate lung and blood pool [$C_p(t) = C_\alpha e^{-\lambda_\alpha t} + C_\beta e^{-\lambda_\beta t} + C_\gamma e^{-\lambda_\gamma t}$], based on the ancillary rule of lumping (*MTT* ratio of 2). In this comparison, we found that the fold-change in the initial slope ($\lambda_\alpha{}'/\lambda_\alpha$) was directly proportional to the ratio of $MTT_c/MTT_c{}'$ as shown in Supplementary Fig. S8. Furthermore, this relationship was obtained without significant alterations in the ratios of slopes for distributional ($\lambda_\beta{}'/\lambda_\beta$) and terminal ($\lambda_\gamma{}'/\lambda_\gamma$) phases. These observations indicate that the slope at time 0 (e.g., $\sum C_i\lambda_i/C_0$), which is mathematically associated with the change of MTT_c [23], is mostly governed by the initial slope λ_α (see also x-intercept for the right-hand side of Eqs. 11 and 12). Therefore, if a rapid decline of plasma concentration profiles in the initial phase is of great importance, it would be useful to monitor the change in MTT_c that could lead to a significant alteration of the initial phase slope in model simulations when the lung and blood pool are being lumped as a single group. In the lumping of the lung into the blood pool of Model C, however, some drugs with extremely high permeability coefficients; e.g., colistin methanesulphonate, colistin sulfate, diltiazem, and epigallocatechin-3-gallate; showed deviations between $\lambda_1{}'/\lambda_1$ and $MTT_c/MTT_c{}'$ (Supplementary Fig. S5). Therefore, we utilized Model C to compare with simplified model structures where the blood pool consisted of just artery and vein while the lung was regarded as one of the peripheral tissues in the subsequent calculations.

K_{det}, a crucial factor governing the number of tissue groups, was theoretically defined in our companion paper [10] and its practical threshold was determined in this study. In particular, we studied the impact of the progressive lumping of tissues in the direction from the tissue with the longest *MTT* (i.e., MTT_{max}) on *FCT* [i.e., $(\lambda_{ter}{}' - \lambda_{ter})/\lambda_{ter}$]. From Taylor series expansions of Eqs. 11 and 12 in the companion paper [10], it was found that *FCT* could be mathematically approximated as ${K_{det}}^2 \cdot UET_{SEG}$ (Eq. 2). In practice, however, the relationship between *FCT* and ${K_{det}}^2 \cdot UET_{SEG}$ could be

much more complex; this is especially true when the difference between $O((MTT\lambda)^2)$ (i.e., the second-order error term by the lumping of SEG, when Eqs. 11 and 12 were expanded) and UET_{SEG} became significant. In fact, the relationship between FCT and UET_{SEG} (Fig. 3a) appeared to more closely follow an exponential relationship (Eq. 10), rather than a simple linear relationship:

$$FCT = \frac{\lambda_{ter}{}' - \lambda_{ter}}{\lambda_{ter}} \cong e^{K_{det}{}^2 \cdot UET_{SEG}} - 1 \quad (10)$$

We were not able to identify the mathematical basis for this apparent relationship, although the estimates of K_{det} were quite consistent with the ratio of MTT_{max} and MRT_B (Supplementary Fig. S9) when the actual calculations from our literature examples were fitted to Eq. 10. For the purpose of this study, however, we were only interested in FCT values of 0.1 or less and, thus, the error would be negligible even when FCT was assumed to be directly related to $K_{det}{}^2 \cdot UET_{SEG}$. The consideration of an exponential relationship between FCT and UET_{SEG} (Eq. 10) may not be practically necessary here. When the values of MTT_{max} (e.g., estimated value based on anatomical/physiological variables and predicted/measured K_p, f_d, and R) and MRT_B (e.g., standard moment analysis) were evaluated, the robustness of FCT as a determinant for the lumping of tissues into the SEG may be estimated by the determination of K_{det}. It should also be noted that, based on the apparent relationship shown in Eq. 10, a slight deviation of the fitted K_{det} from MTT_{max}/MRT_B (Supplementary Fig. S9) could occur when the value exceeded 10 (i.e., 16.4% of total points). However, the appropriateness of the relationship $K_{det} = MTT_{max}/MRT_B$ as the determining coefficient for the number of tissue groups would still apply since, as described in Fig. 3a, this large value of K_{det}, e.g. > 10 would essentially lead to the marked change in FCT (i.e., sensitive to UET_{SEG}) and thus the corollary use of another tissue group of different distribution rate, namely, the REG would be appropriate.

In this study, we proposed that the compounds having $K_{det} < 0.3$ can be reasonably classified as representing a one-tissue model. In the literature, Pilari and Huisinga [24] studied the pharmacokinetics of 25 compounds and determined that only 5 drugs were considered to follow the one-tissue model because of their relatively low MTT_{max} values. However, when the criterion of K_{det} proposed here was applied to the same 25 compounds studied by Pilari and Huisinga, a total of 16 drugs may be categorized to follow the one-tissue model. This discrepancy may arise because the authors considered similarity in the concentration-time profiles of all tissues, some of which may not significantly contribute to the systemic pharmacokinetics. The objective of our study was to provide a theoretical basis for the simplification of WB-PBPK model (Model C) to reduced models (Model D/E) without affecting the plasma pharmacokinetic profiles, rather than reproduce all tissue concentration-time profiles, of the compound being studied.

While most compounds where $FCT < 0.1$ showed comparable values between λ_β and λ_{major} for $K_{det} > 1$ (Supplementary Fig. S10a) calculated from all the possible combinations of SEG and REG, we found that certain compounds with $0.3 \le K_{det} < 1$ (i.e., 301 out of 504 cases) had $\lambda_\beta/\lambda_{major}$ values exceeding a factor of 2 (Supplementary Fig. S10b). The dissociated $\lambda_\beta/\lambda_{major}$ factor for these compounds indicates that the lumping of tissues into the REG may not be appropriate for these compounds. In this study, we did not directly examine the kinetic/biopharmaceutical reason(s) for the dissociation. However, it could be speculated that the presence of structural error, e.g., the presence of kinetically ambiguous tissue(s) and/or inadequacy of setting up a single "major" tissue representing λ_β, might be involved in causing the discrepancy under this condition of $0.3 \le K_{det} < 1$. Unfortunately, the rearrangement of the order of tissues rather than the descending order of MTT (e.g., based on the capability of a candidate tissue for obtaining the minimal UET_{SEG} value when lumping from the longest tissue) did not improve the dissociation between λ_β and λ_{major} for these compounds. Despite this limitation, however, it would be noteworthy that the contribution of S_{rec} to AUC was found to be less than 19% for drugs of $0.3 \le K_{det} < 1$ (Fig. 4b). Therefore, a significant deformation between Models C and D and/or a significant inadequacy of λ_{major} appeared less likely. For the sake of practicality, for those compounds of $0.3 \le K_{det} < 1$, it is possible that λ_β may be slightly deviated from λ_{major} despite the fact that the contribution of the deviation could be minor to the overall AUC. If necessary, this deviation of λ_β from λ_{major} could be estimated by the use of UET_{REG} (Fig. 5b) [10]. When the pharmacokinetic profile in this phase is of great importance, the use of Model C may be appropriate.

Despite some of such potential deviations in the distributional-phase slopes during the lumping, a reasonable correlation in $f_{d,lum}$ values between bottom-up calculations by Eq. 1b and top-down fitting of Eq. 9a and 9b to the errorless dataset (Fig. 6a) indicated the appropriateness of the current lumping method. According to the currently available tissue lumping methods in the literature [22, 24–27], visual/numerical assessments were often considered to evaluate the appropriateness of tissue lumping, as also shown in this study (Supplementary Material 2). In addition, statistical evaluation could be also useful for comparisons between WB-PBPK and lumped models [e.g., the prediction error $PE = \log C_{pred} - \log C_{obs}$ [26]; analogous to Eqs. 6 and 7]. However, since our tissue lumping method was derived on the basis of a symbolic approach, the endpoint criterion for assessing the adequacy of tissue lumping could now be improved to include the simple comparisons of lumped PBPK model parameters, e.g., $f_{d,lum}$ in this study (Fig. 6a).

Based on calculations for the 113 model compounds, it was readily apparent that the distributional phases in terms of plasma pharmacokinetics for the compounds of $K_{det} \geq 5$ were clearly distinct as evidenced by tissue *MTT* values [e.g., for metformin, K_{det} value was 7.10 for rats where MRT_B, MTT_{SEG} and MTT_{REG} values were 23.1, 164, and 13.4 min in mPBPK models [28]]. In contrast, for compounds with lower K_{det} values, e.g., $0.3 \leq K_{det} < 1$, the distinction between MTT_{SEG} and MTT_{REG} was less apparent, indicating that certain tissue(s) may partially participate in both REG and SEG, as evidenced by some deviations between theoretical and fitted f_d values for indomethacin and ochratoxin (Fig. 6a; Supplementary Table SIII).

In this study, the model difference calculated from Eq. 7 was assumed to be practically acceptable under a factor of 2 (i.e., $y < 1$): Despite the fact that determination of an adequate acceptance level of model difference may be difficult to theoretically set, we found that the model difference y could be related as a function of *FCT* (Fig. 2) where the *FCT* less than 0.1 was associated with a 2-fold error (i.e., $y < 1$). Using perchloroethylene as an example, visual/numerical inspections (Supplementary Material 2) showed indistinguishable profiles between Model D and WB-PBPK models, yet the model difference y was approximately 0.933, a value close to 1 (i.e., 2-fold error), supporting the practical utility of the current conditions (i.e., $y < 1$ and $FCT < 0.1$) of SEG lumping.

However, slight deviations between Models D and A/B/C (Supplementary Material 2) were noted in plasma pharmacokinetic profiles for some compounds (i.e., biochanin A, bisphenol A, genistein, glycyrrhetic acid, ipriflavone, paclitaxel, parathion, and propofol). Due to their K_{det} values ranging from 3.53 to 73.8, only one tissue (i.e., skin) was capable of being lumped into the SEG (Supplemental Table SIII) while the second-largest tissue (i.e., adipose) and the remaining ones were lumped into the REG (cf. MTT_{AD}/MTT_1 ranging from 51.7 to 82.7 for the 8 compounds). Since such high K_{det} values would lead to emergence of distinct distributional/terminal phases in plasma profiles depending on the *MTT*s of WB-PBPK tissues (Supplementary Table SIV), more than 2 tissue groups (e.g., skin, adipose, and the REG) could have been utilized to reproduce all the exponential phases arising from divergent/distinct tissue transit times for those compounds, as evidenced by Supplementary Fig. S11. Despite the practical applicability of the general premise of this study (i.e., WB-PBPK models being represented as bi- or tri-exponential functions) wherein the current lumping criteria (i.e., $y < 1$ and $FCT < 0.1$) were applied for the model compounds, cautions would be required especially when Model C could possibly be described by more than 3 exponential terms (i.e., $K_{det} > 1$).

In typical mammillary two-compartment models, the shape of the plasma concentration profile was reported to be dependent on the number of cycles around the central compartment (i.e., CL_D/CL_{sys}) [29]. When $CL_D < CL_{sys}$, the terminal phase kinetics was considered to be distribution-limited. This concept of the ratio CL_D/CL_{sys} in the literature could be also applied to WB-PBPK. Equation 11 showed that the theoretically possible maximum of λ_{ter} would be $1/MTT_{max}$. The CL_D in the two-compartment model would be analogous to $\sum Q_T f_d$ in the WB-PBPK structure. Where $CL_D < CL_{sys}$, viz., $Q_9 f_{d9} < CL_{sys}$ here [30], it was observed that a sufficiently large systemic clearance could result in λ_{ter} being approximated to be the reciprocal of the longest *MTT* tissue in WB-PBPK. In many typical pharmacokinetic studies, however, the kinetics in the terminal phase may often remain unaccounted at the last sampling time, most likely due to limitations in the analytical quantification method. From our in silico calculation (e.g., wherein the limitation of sampling times was eliminated), we found that the tissue with the longest *MTT* was, in most cases (110 out of 113), the skin (exceptions, the brain for chlorzoxazone, muscle for colistin sulfate, and adipose for tamoxifen). The reciprocal of the maximum *MTT* value for 9 peripheral tissues was highly correlated with λ_{ter}, the smallest eigenvalue of WB-PBPK (e.g., 68.1% and 71.7% within a factor of 2, for Models 1 and 2) (Supplementary Fig. S12). Therefore, it may be worth attempting a priori calculation of *MTT* values for various tissues in order to ascertain the possibility of the existence of a kinetically deep tissue compartment (e.g., skin tissue) that could be overlooked in the systemic pharmacokinetics [31].

Conclusions

In summary, we herein propose a biopharmaceutical condition for determining the number of tissue groups in simplified forms of WB-PBPK models. For $K_{det} < 0.3$, the use of Model E (i.e., blood pool plus one lumped peripheral tissue) could be adequate since the *FCT* would be less than 0.1 even with all peripheral tissues collectively lumped and the S_{rec}/AUC ratio would be less than approximately 2%. For $K_{det} \geq 1$, the tissue with MTT_{max} could be progressively lumped with the shorter *MTT* tissue(s) into the SEG, provided that *FCT* was less than 0.1. The remaining tissues could then be lumped into the REG (Model D; blood pool plus two lumped tissue groups with different equilibrating rates). Our primary recommendation for the cases of $0.3 \leq K_{det} < 1$ was to cautiously apply the same rule of the case of $K_{det} \geq 1$ (i.e., Model D), considering the fact that the contribution of the distributional area S_{rec} to the *AUC* was less than approximately 19%. Despite some of such potential deviations in the

distributional-phase slopes during the lumping, our tissue lumping method based on a symbolic approach allowed a simple comparison of lumped PBPK model parameters, e.g., $f_{d,lum}$ in this study, whereby a consistent correlation indicated the appropriateness of the current lumping method. Collectively, by using the principles proposed in this study, WB-PBPK could be simplified to mPBPK models without significantly affecting plasma concentration-time profiles. Furthermore, the current approach may enable theoretical calculation of key coefficients of mPBPK models using estimates from in silico/in vitro studies.

Appendix

By applying Gauss elimination of the system matrix A of PBPK Model C [10], 10 eigenvalues were readily determined using Eq. 11:

$$\frac{\frac{Q_1 f_{d1}}{MTT_1}}{\lambda - \frac{1}{MTT_1}} + \frac{\frac{Q_2 f_{d2}}{MTT_2}}{\lambda - \frac{1}{MTT_2}} + \cdots + \frac{\frac{Q_9 f_{d9}}{MTT_9}}{\lambda - \frac{1}{MTT_9}} = V_B\left(\lambda - \frac{1}{MTT_c}\right) \tag{11}$$

When the two-tissue mPBPK model (Model D) is applicable, the eigenvalues (in terms of λ'; the roots corresponded to λ_α, λ_β, and λ_γ) after tissue lumping could be determined by Eq. 12:

$$\frac{\frac{Q_{SEG} f_{d,SEG}}{MTT_{SEG}}}{\lambda' - \frac{1}{MTT_{SEG}}} + \frac{\frac{Q_{REG} f_{d,REG}}{MTT_{REG}}}{\lambda' - \frac{1}{MTT_{REG}}} = V_B\left(\lambda' - \frac{1}{MTT_c}\right) \tag{12}$$

Supplementary Information The online version contains supplementary material available at https://doi.org/10.1208/s12248-022-00733-x.

Author Contribution Yoo-Seong Jeong: Conceptualization, methodology, formal analysis, investigation, data curation, writing-original draft, writing-review & editing, visualization

Min-Soo Kim: Methodology, software, formal analysis, data curation, writing-review & editing, visualization

Suk-Jae Chung: Conceptualization, methodology, formal analysis, writing-original draft, writing-review & editing, supervision, project administration, funding acquisition

Funding This study was supported by the Korea Environment Industry & Technology Institute (KEITI) through the project for BioMarkers TRANSLation of consumer chemicals/ft.life-stage PBPK modeling (BioTranSL/PBPK) (NO. 2022002970003).

Declarations

Conflict of Interest The authors declare no competing interests.

References

1. Levy G, Gibaldi M, Jusko WJ. Multicompartment pharmacokinetic models and pharmacologic effects. J Pharm Sci. 1969;58(4):422–4.
2. Benet LZ. General treatment of linear mammillary models with elimination from any compartment as used in pharmacokinetics. J Pharm Sci. 1972;61(4):536–41.
3. Cao Y, Jusko WJ. Applications of minimal physiologically-based pharmacokinetic models. J Pharmacokinet Pharmacodyn. 2012;39(6):711–23. https://doi.org/10.1007/s10928-012-9280-2.
4. Sager JE, Yu J, Ragueneau-Majlessi I, Isoherranen N. Physiologically based pharmacokinetic (PBPK) modeling and simulation approaches: a systematic review of published models, applications, and model verification. Drug Metab Dispos. 2015;43(11):1823–37.
5. Riegelman S, Loo J, Rowland M. Shortcomings in pharmacokinetic analysis by conceiving the body to exhibit properties of a single compartment. J Pharm Sci. 1968;57(1):117–23.
6. Hirtz J. The fate of drugs in the organism. A bibliographic survey complied by the Societe´ Fran¸aise des Sciences et Techniques Pharmaceutique, Working group under the chairmanship of HIRTZ. Dekker New York; 1974.
7. Segre G. Pharmacokinetics—compartmental representation. Pharmacol Ther. 1982;17(1):111–27.
8. Vaughan D, Dennis M. Number of exponential terms describing the solution of an N-compartmental mammillary model: Vanishing exponentials. J Pharmacokinet Biopharm. 1979;7(5):511–25.
9. Wagner JG. Linear pharmacokinetic models and vanishing exponential terms: Implications in pharmacokinetics. J Pharmacokinet Biopharm. 1976;4(5):395–425.
10. Jeong Y-S, Kim M-S, Chung S-J. Determination of the number of tissue groups of kinetically distinct transit time in whole-body physiologically-based pharmacokinetic (PBPK) models I: Theoretical consideration of bottom-up approach of lumping tissues in whole-body PBPK. AAPS J. 2022. https://doi.org/10.1208/s12248-022-00732-y.
11. Lobell M, Sivarajah V. In silico prediction of aqueous solubility, human plasma protein binding and volume of distribution of compounds from calculated pKa and AlogP98 values. Mol Diversity. 2003;7(1):69–87.
12. Jamei M, Marciniak S, Feng K, Barnett A, Tucker G, Rostami-Hodjegan A. The Simcyp® population-based ADME simulator. Expert Opin Drug Metab Toxicol. 2009;5(2):211–23.
13. Colclough N, Ruston L, Wood JM, MacFaul PA. Species differences in drug plasma protein binding. Med Chem Commun. 2014;5(7):963–7.
14. Uchimura T, Kato M, Saito T, Kinoshita H. Prediction of human blood-to-plasma drug concentration ratio. Biopharm Drug Dispos. 2010;31(5-6):286–97. https://doi.org/10.1002/bdd.711.
15. Kerns EH, Di L, Petusky S, Farris M, Ley R, Jupp P. Combined application of parallel artificial membrane permeability assay and Caco-2 permeability assays in drug discovery. J Pharm Sci. 2004;93(6):1440–53.
16. Fujikawa M, Ano R, Nakao K, Shimizu R, Akamatsu M. Relationships between structure and high-throughput screening permeability of diverse drugs with artificial membranes: application to prediction of Caco-2 cell permeability. Bioorg Med Chem. 2005;13(15):4721–32. https://doi.org/10.1016/j.bmc.2005.04.076.
17. Jeong Y-S, Yim C-S, Ryu H-M, Noh C-K, Song Y-K, Chung S-J. Estimation of the minimum permeability coefficient in rats for perfusion-limited tissue distribution in whole-body physiologically-based pharmacokinetics. Eur J Pharm Biopharm. 2017;115:1–17.
18. Rodgers T, Leahy D, Rowland M. Physiologically based pharmacokinetic modeling 1: Predicting the tissue distribution of

moderate-to-strong bases. J Pharm Sci. 2005;94(6):1259–76. https://doi.org/10.1002/jps.20322.
19. Rodgers T, Rowland M. Physiologically based pharmacokinetic modelling 2: predicting the tissue distribution of acids, very weak bases, neutrals and zwitterions. J Pharm Sci. 2006;95(6):1238–57. https://doi.org/10.1002/jps.20502.
20. Øie S, Tozer TN. Effect of altered plasma protein binding on apparent volume of distribution. J Pharm Sci. 1979;68(9):1203–5.
21. Brown R, Delp M, Lindstedt S, Rhomberg L, Beliles R. Physiological parameter values for physiologically based pharmacokinetic models. Toxicol Ind Health. 1997;13407:407–84.
22. Nestorov IA, Aarons LJ, Arundel PA, Rowland M. Lumping of whole-body physiologically based pharmacokinetic models. J Pharmacokinet Biopharm. 1998;26(1):21–46.
23. Veng-Pedersen P, Gillespie WR. Single pass mean residence time in peripheral tissues: a distribution parameter intrinsic to the tissue affinity of a drug. J Pharm Sci. 1986;75(12):1119–26.
24. Pilari S, Huisinga W. Lumping of physiologically-based pharmacokinetic models and a mechanistic derivation of classical compartmental models. J Pharmacokinet Pharmacodyn. 2010;37(4):365–405.
25. Gueorguieva I, Nestorov IA, Rowland M. Reducing whole body physiologically based pharmacokinetic models using global sensitivity analysis: diazepam case study. J Pharmacokinet Pharmacodyn. 2006;33(1):1–27.
26. Björkman S. Reduction and lumping of physiologically based pharmacokinetic models: prediction of the disposition of fentanyl and pethidine in humans by successively simplified models. J Pharmacokinet Pharmacodyn. 2003;30(4):285–307.
27. Brochot C, Tóth J, Bois FY. Lumping in pharmacokinetics. J Pharmacokinet Pharmacodyn. 2005;32(5-6):719–36.
28. Jeong Y-S, Jusko WJ. Meta-assessment of metformin absorption and disposition pharmacokinetics in nine species. Pharmaceuticals. 2021;14(6):545.
29. Kong AN, Jusko WJ. Definitions and applications of mean transit and residence times in reference to the two-compartment mammillary plasma clearance model. J Pharm Sci. 1988;77(2):157–65.
30. Berezhkovskiy LM. Prediction of drug terminal half-life and terminal volume of distribution after intravenous dosing based on drug clearance, steady-state volume of distribution, and physiological parameters of the body. J Pharm Sci. 2013;102(2):761–71.
31. Fleishaker JC, Smith RB. Compartmental model analysis in pharmacokinetics. J Clin Pharmacol. 1987;27(12):922–6.